J Am Oil Chem Soc (2010) 87:133–145
DOI 10.1007/s11746-009-1476-2

ORIGINAL PAPER

Effect of Cooling Rate on the Structural and Moisture Barrier Properties of High and Low Melting Point Fats

Claire Bourlieu · Valérie Guillard · Mariana Ferreira · Hugh Powell · Baltasar Vallès-Pàmies · Stéphane Guilbert · Nathalie Gontard

Received: 7 July 2009 / Revised: 8 September 2009 / Accepted: 13 September 2009 / Published online: 26 September 2009

Abstract The effect of three cooling rates (rapid, intermediate and slow CR) on the moisture barrier properties and on the physical state of acetylated and high melting point hydrophobic self-supported moisture barriers has been investigated. The selected CR were representative of industrial processing conditions and the selected barrier materials of common effective GRAS substances (acetomonopalmitin, white beeswax, two commercial blends of beeswax and acetylated glycerides and a blend of palmitic/stearic acids). Variations of CR affected crystallisation kinetics, SFC in an extend depending on the fat chemical composition and degree of undercooling, crystal size and ratio of polymorphs present in the materials. It did not have major influence on the contact angles with water measured at the surface of the materials and on the mass–volume area properties of the material. The resultant effect on the macroscopic moisture barrier properties of the materials were evaluated using water vapour permeability (WVP) measurements. The CR had no significant effect on the WVP, except for one blend of acetylated fat and beeswax for which a slow CR may have favoured the healing of imperfections. The variations of WVP between all materials and CRs were mainly attributed to variation in materials polarity using multivariable analysis.

Keywords Lipid barriers · Water vapour permeability · Cooling rate · X-ray diffraction · Solid fat content · Mass–volume area related properties

C. Bourlieu · V. Guillard · M. Ferreira · S. Guilbert · N. Gontard
UMR 1208 Ingénierie des Agropolymères et Technologies Emergentes, CIRAD, INRA, Montpellier SupAgro, Université Montpellier 2, 34000 Montpellier, France
e-mail: claire.bourlieu@rennes.inra.fr

H. Powell
Science Group, Nestlé Product Technology Centre, York (Nestec York Ltd), York, UK

B. Vallès-Pàmies
Liquid Products, Nestlé Research Center, Lausanne, Switzerland

Present Address:
C. Bourlieu
UMR 1253 STLO, 35000 Rennes, France

V. Guillard (✉)
UMR IATE, Université de Montpellier II, Bat 15. 4° étage CC 023, Place E. Bataillon, 34095 Cedex 05 Montpellier, France
e-mail: guillard@univ-montp2.fr

Abbreviations

AMP	Acetomonopalmitin
CR	Cooling rate
d_{app}	Apparent density
d_{true}	True density
GRAS	Generally recognised as safe
MP	Melting point
P/S	Palmitic/stearic acid blend
RH	Relative humidity
SEM	Scanning electron microscopy
SFC	Solid fat content
W/A	Wax/acetic acid ester of mono and diglycerides
WVP	Water vapour permeability
XRD	X-ray diffraction

List of symbols

A	Area of exposed film
α, β', β	Hexagonal, orthorhombic and triclinic subcell lateral packings
d	Interplanar crystal lattice distance

Δ_s	Slope of water weight versus time
e	The film thickness
ε	Porosity
k	Avrami constant
M	Molecular mass of water
n	Avrami exponent or index of crystallisation
p°	the saturating water vapour pressure of water at constant considered temperature
a_w	Water activity

Introduction

Edible moisture barriers usually include lipids in their formulation. Because of their apolar nature, these hydrophobic substances are capable of forming water-impervious structures and efficiently reduce water transfer. The efficacy of the moisture barriers of lipids is related to their chemical composition (presence of polar components, hydrocarbon chain length, number of unsaturation(s), geometric configuration of unsaturation(s) and acetylation…) at constant temperature. For components having the same chemical nature, increasing chain length modifies the barrier properties because the polar part of the molecule decreases and does not favour water solubility in the film [1]. Thus 'waxes' based on esters of monohydroxy long chain alcohols and long chain fatty acids, which are characterised by an extremely reduced hydrophilic part, are considered the most effective moisture barriers. Among waxes, beeswax has been widely studied. Indeed, beeswax presents a relative flexibility in relation to its viscoelastic behaviour [2] and is an authorised edible coating ingredient with no other limit than the Good Manufacturing Practices on the American and European markets. Carboxylic acids and glycerides are other common hydrophobic barrier-forming derivatives. For such compounds, moisture barrier efficacy increases with carbon number, up to 16–18 carbons, and then decreases due to the heterogeneous structure within the material [3]. Specific attention has thus been given to palmitic and stearic acids, though efficacy of such derivatives is limited by poor mechanical properties. Acetylated glycerides have also been frequently presented as good moisture barriers due to their good mechanical properties, high oxidative stability and low melting point [4–6].

The barrier efficacy of lipids is also influenced by their solid fat content (SFC): positive correlations between SFC and moisture transfer resistance of fat, up to a given threshold after which mechanical properties of the fat deteriorate, have been reported in various studies [3, 7].

The crystal habit of lipids (polymorphism, crystallite size and shape, spatial distribution of the network mass) may also affect their barrier efficacy. However, no clear consensus has been reached on the effect of lipid crystal polymorphism on water transport through barrier films. The three main forms of crystallisation of triglycerides, in increasing order of thermodynamic stability and hydrocarbon chain packing, are: α (hexagonal), β' (orthorhombic) and β (triclinic). It could be expected that the β form which is the densest and best ordered would present the highest moisture transfer resistance. This favourable influence of a more stable polymorph was reported by Lovegren et al. [8] and Landman et al. [9], respectively, on 1,2-diaceto-3-stearin and cocoa butter. However, none of these authors analysed precisely the polymorphic forms present. Conversely, Kester and Fennema [10] found that a change from β' form to α form induced a decrease in the WVP value for a blend of hydrogenated rapeseed and soybean oils. The better efficacy of the α form was explained by the higher flexibility induced by smaller crystal size which limited defect formation during crystallisation. Donhowe and Fennema [11] studied the WVP of various natural waxes and reported that these waxes presented a mixture of β' and α crystals. These authors concluded that the differences in values of WVP between the different types of waxes were more likely due to variations in the amount of hydrophilic compounds contained in the waxes than to the difference in polymorphic forms.

SFC and the crystals habits of lipid films are themselves strongly affected by heat, mass and momentum transfer during the crystallisation process, i.e. during the film shaping procedure. CR, shearing and degree of undercooling correspond to the three key factors generally modified to modulate SFC and fat crystals habit [12]. Comparisons of CRs showed that a slow crystallisation process leads to a decrease in SFC as well as to the aggregation of small crystalline particles into larger ones and can favour the formation of more stable polymorphs [13]. Despite this impact of CR on lipid-based moisture barrier properties, only few integrated approaches relating CR, microstructural level and macroscopic barrier properties of lipid-based film, have been proposed in the scientific literature. In one of the earliest studies [13], only crystal morphology and size along with the resulting water vapour transmission rate of paraffin wax-coated cellophane were considered. These authors noticed an important effect of the CR on the crystalline structure of the wax: shock cooling the wax in cold water gave rise to small unoriented wax crystals. Such crystallisation conditions led to high water vapour transmission rate material possibly due to the presence of small crystallites, numerous paths around crystallites and microscopic structural defects in the material. Subsequent storage of the fat films at high temperature resulted in improved water resistance of the

coating. This positive effect was confirmed later on using stearyl alcohol-based film [14] and explained by modifications of size and shape of crystals, by healing of microscopic structural defects, and by a possible SFC increase during storage. More recently, the effect of processing conditions (3 CRs: 50, 30, 10 °C/min without shearing and 1 intermediate CR with shearing) on the structure, physico-chemical properties and WVP of 4 low melting point (MP) fats (MP ~33 °C, distilled monoglyceride/canola oil, partially hydrogenated palm kernel oil/canola oil, partially hydrogenated palm kernel oil/canola oil/emulsifier, Benefat®) have been discussed by Martini et al. [15, 16]. Processing conditions affected the microstructure of the two fats containing hydrogenated palm kernel oil but not of the two others. Processing conditions did not significantly affect the WVP of the fat samples. However, the crystal domain size (influenced by crystallisation conditions for some of the fats) and SFC were pointed out as major factors controlling water vapour transfer through the barrier.

Therefore, the objective of the present study was to analyse further the influence of CR on edible barriers physical and moisture properties. In this aim, the effect of variable CRs, representative of fat barrier possible conditions of application on an industrial scale, on commonly used barrier-forming materials, i.e. high MP or acetylated fats, was studied. The consequence of variable CRs was investigated at several scale levels: from the crystalline properties of the material (SFC, crystal habits) to their mesoscopic properties (contact angle with water) and eventually macroscopic mass–volume related properties (true and apparent density, water barrier properties).

Materials and Methods

Fat Materials

Five lipid derivatives were selected as representative of common and effective lipid-film forming derivatives. The derivatives presented variable chemical composition and melting range which are summarised in Table 1.

Conditions of Crystallisation

Samples of fat materials were melted at 10 °C above their MP for at least 10 min in order to destroy any crystal memory with magnetic stirring (100 rpm). The materials were then cast with a thin layer spreader and solidified on a levelled iron plate, presenting important thermal inertia, whose temperature had been adjusted to:

1. 5 °C, this crystallisation procedure will be abbreviated as Rapid CR (initial CR estimated to be 20 °C/min over the first minute of crystallisation).
2. 20 °C, this crystallisation procedure will be abbreviated as Intermediate CR (initial average CR estimated to be 7 °C/min over the first 4 min of crystallisation).
3. 45 °C, this crystallisation procedure will be abbreviated as Slow CR (average CR estimated to be 0.15 °C/min).

Due to the variations in the melting range of the selected fats, the CR-applied induced a variable degree of undercooling in the material, but these conditions are in adequation with fixed coating-forming industrial process.

After 120 min of crystallisation on the levelled iron plate at 20 °C, the films were detached from the plate and transferred for 48 h to a thermoregulated cabinet (20 °C) to complete the crystallisation process before being used for subsequent analysis.

Crystal Morphology

A small amount (5 mg) of the sample, was placed on a glass slide, heated rapidly to 10 °C above the melting point of the fat and covered with a similarly preheated coverslip. The coverslip was placed parallel to the plane of the slide and centered on the drop of sample to ensure that the sample thickness was uniform. The slide was immediately transferred onto the levelled iron plate to follow crystallisation procedures (1), (2) or (3).

Polarised light micrographs were obtained using a 200× and a 400× objective using a polarised light microscope (Leica-Leitz DM RPX, Leica Microsystems, France) and Leica Application Suite Microsystems software. The observations were conducted in triplicate.

Scanning Electron Microscopy (SEM)

The microstructure of the shaped films was observed by SEM (JSM-6300 F, Japan). The samples were mounted on 13-mm diameter aluminium stubs using doubled-sided adhesives tape and coated with 5–10 nm thick metal (platinum, coating time 100 s). The stubs were flat for surface observations and presented at a 45° angle for cryofracture cross-observations. Samples for cross-observations were fractured by immersion of the extremity of a 50 × 20 mm film sample in liquid nitrogen. All samples were scanned by a focussed electron beam (3–5 kV) and secondary electrons were processed to form enlarged images. Due to low MP and sensitivity, AMP samples could not be observed.

Table 1 Summary of the characteristics of the film-forming fat materials studied

Name of fat material	Abbreviation	Melting point (°C)	Chemical composition	Supplier
White beeswax	(–)	62–65	Ester value = 72–79, acid value = 17–24	Fisher Bioblock Scientific, Illkirch, France
Blends of white beeswax and acetic acid ester of mono and diglycerides (GBS 1000® and GBS 2000®)	W/A 1, W/A 2	57	Fatty acid chain length of ACETEM = C16/C18, White beeswax addition ≤20% w/w	Danisco Ingredients, 78000 Trappes, France
Palmitic-stearic acids blend	P/S acids blend	54–57	41–51% w/w GC Stearic acid; 49–54% w/w GC palmitic acid	Fluka, Sigma-Aldrich, France
Acetylated monopalmitin (TSED 619®)	AMP	30	Fatty acid chain length = C16, percentage of free hydroxyl groups acetylated = 70%	Danisco Ingredients, 78000 Trappes, France

X-Ray Diffraction (XRD)

Fat polymorphism was determined by X-ray diffraction using a PHILIPS X'Pert MPD diffractometer ($\theta-2\theta$), equipped with the X'celerator detector, using the Cu K_α radiation ($\lambda = 1.5418$ Å) generated at 40 kV/20 mA and a nickel filter. A glass sample holder (ca. 20 mm × 30 mm) was used in reflection geometry. Data gathering was performed in continuous mode for 2θ angles ranging from 10° to 40° with a scan rate of 2°/min. Peak detection and analysis were performed by means of the X'pert Highscore software without baseline subtraction.

SFC Determination

The crystallisation behaviour of the samples was studied by measuring the development of solid crystalline material as a function of time. Glass NMR tubes (10 mm outside diameter) were filled with approximately 3 g of sample and heated up to a temperature of 80 °C for 30 min. The NMR tubes were then immersed in water baths: either set at a given temperature corresponding to the intermediate or rapid CR (20 °C and 5 °C) or submitted to a simplified CR (44.0 °C for 5 min, 38.8 °C for 26 min, 33.0 °C for 29 min, 28.5 °C for 23 min, end of cooling procedure at ambient temperature i.e. 20 ± 2 °C) thanks to a set of heating blocs. SFC (%) measurements were taken at suitable time intervals by pulsed Nuclear Magnetic Resonance (Minispec 120, Bruker). Two replicate determinations were performed to determine non-equilibrium SFC and 6 replicate determinations were performed to determine SFC at equilibrium designed as SFC_∞ (after 48 h).

Crystallisation curves were constructed from these data by plotting the SFC (%) as a function of time (up to 156 min). The crystallisation curves were fitted to the Avrami model by non-linear regression. The Avrami model has the form of:

$$\frac{SFC(t)}{SFC_{max}} = 1 - e^{kt^n} \quad (1)$$

where SFC(t) is the SFC(%) as a function of time, SFC_{max} is the maximum SFC attained, the Avrami constant (k, min^{-n}) represents the crystallisation rate constant, and the Avrami exponent or index of crystallisation (n) indicates the crystal growth mechanism. This index is a combined function of time dependence of nucleation and the number of direction in which the growth takes place. Experimental induction times of crystallisation were determined from SFC-time curves by extrapolating back to the onset time of linear SFC increase. It should be noted however, that strict application of the Avrami models supposes isothermal conditions and that the identified parameter during this crystallisation process under non-equilibrium, non isothermal conditions are only apparent.

Thermal Behaviour

The melting behaviour of the samples was monitored using Differential Scanning Calorimetry (DSC 2920, TA Instruments, Guyancourt, France). Approximately 12 mg of melted sample obtained using the three previous CRs were introduced into standard DSC aluminium pans and then hermetically sealed. The DSC was set to 5 °C and analyses were performed from this temperature up to 80 °C at a heating rate of 5 °C/min. Liquid nitrogen was used as the cooling medium and an empty and hermetically sealed DSC aluminium pan was used as reference. Peak melting temperatures were calculated using the TA analysis 2000 software.

True Density of the Material

The true density (d_{true}) of the shaped barrier was estimated using helium stereopycnometer SPY-6DC (Quantachrome

Instruments, Florida, USA). A sample of self-supported film of 2 g was folded and inserted in the measuring cell (33.43 cm^3, calibration volume 56.56 cm^3). The true volume was deduced by applying Archimedes' and Boyle's law.

Apparent Density

The apparent density (d_{app}) of the shaped barrier was measured using the liquid displacement method. The volume of a small neck specific gravity bottle was determined at ambient temperature using distilled water (25 mL). Each sample was weighted precisely ($\sim$0.3 g) and transferred to the pycnometer half filled with a low viscosity oil. The liquid level was then carefully adjusted with oil. The sample volume was deduced from the difference between the initial and final volume of the oil. The measurements were repeated three times on each sample. The porosity (ε) of the film could be estimated using Eq. 2:

$$\varepsilon = \left(1 - \frac{d_{app}}{d_{true}}\right)100 \quad (2)$$

Contact Angle Measurement

The water contact angle of the fat material was determined using the sessile drop method, i.e. by depositing an ultrapure water droplet (3 μL) with a Digidrop DGD-ASE (GBX, Romans, France) equipped with a CDD camera. The average angle formed by the droplet on the surface of the fat material was monitored over time and considered at metastable equilibrium when this value remained stable for more than 2 s. The measurements were repeated six times for each material.

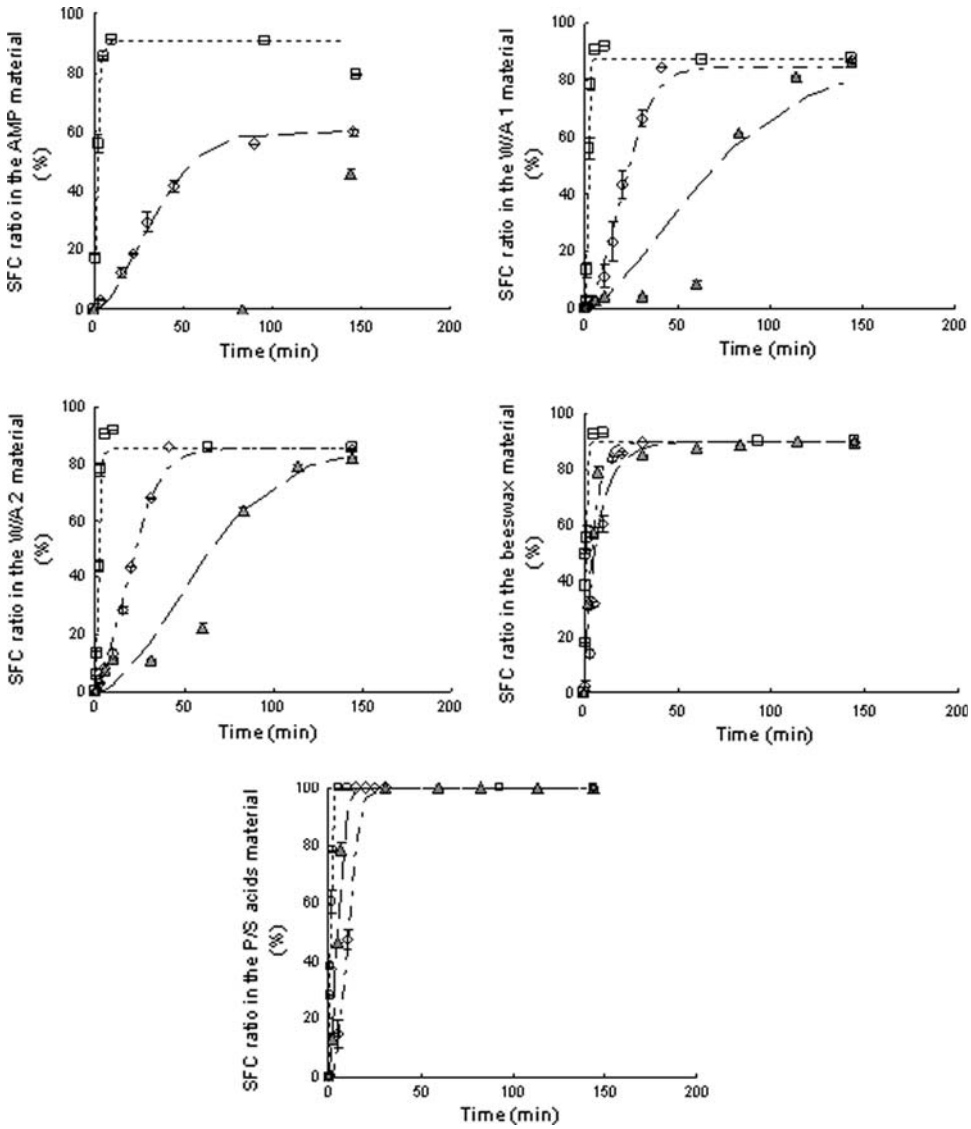

Fig. 1 Evolution of solid fat content (SFC, %) during the crystallisation of the five lipid materials crystallised under different cooling conditions (ambient temperature, two replicates). *Symbols* stand for experimental data with rapid CR (*squares*), intermediate CR (*diamonds*), slow CR (*grey triangles*); the *dotted line* stands for corresponding Avrami fittings

WVP (0–100% RH)

The permeability of the barrier films was determined by a gravimetric method, using a modified procedure (ASTM E96-80; 1986) for a 0–100% relative humidity (RH) difference. The film was sealed on the top of a permeation cell containing distilled water and placed in a desiccator maintained at 20 °C. The desiccator RH was maintained at a theoretical 0% RH with silica gel. The glass permeation cells were 3.4 cm (i.d.), 5.4 cm (o.d.) and 3.4 cm deep with an exposed film area of 9.1 cm^2. The water transferred through the film and was absorbed by the desiccant and the amount was determined from the weight loss of the glass permeation cells. The cups were weighed daily, to the nearest 0.1 mg, over an 8 days period. At least three replicate experiments were carried out for each sample. The slope of the plot of cup weight loss versus time was obtained by linear regression ($r^2 > 0.9$) and water vapour permeability was calculated according to Eq. 3:

$$\mathrm{WVP} = \frac{(\Delta_s e)}{AMp^{\circ}(a_{w1} - a_{w2})} \quad (3)$$

where Δ_s is the slope of weight versus time (g/s), e is the film thickness (m), A is the area of exposed film (m^2), M is the molecular mass of water (g/mol), p° the saturating water vapour pressure of water at constant considered temperature (Pa), $a_{w1}-a_{w2}$ is the water activity difference across the film at the same considered temperature.

The thickness of the films was checked with a hand-held micrometer (Braive Instrument, sensitivity of 0.001 mm) in a cold room (5 °C except for the P/S acids based film which would develop cracks at low temperature) to avoid damaging the samples. Five measurements were made for each type of film and CR.

Multivariate Analysis

Principal Component Multivariate analysis was conducted between the AMP, W/A barriers and White beeswax WVP values and other characteristics (interplanar distance of crystals lattice, surface contact angles, true density, and SFC) using MATLAB® (The Mathworks Inc, Natick, MA, USA) 7.0 PLS Toolbox. This multivariate analysis intended to determine which combination of characteristics could best explain WVP values.

Results and Discussion

Effect of CR on Crystallisation Rate and SFC in the Lipid Materials

SFC evolution versus time in the lipid material is presented on Fig. 1. A significant effect of the CR was observed on the crystallisation kinetics of the systems. This effect was extremely strong for AMP which presented the lowest melting point, intermediate for W/A 1 and W/A 2 and reduced for the White beeswax and P/S acids. Influence of the CR was described using the Avrami model apparent parameters (Table 2). For all fat materials, the crystallisation rate (k) sharply increases between the slow and fast CR. It reveals that the driving force for crystallisation gets higher, as the CR increases, affecting crystal growth and nucleation. Another indicator of crystallisation kinetics is the apparent Avrami exponent (n), both sensitive to the nucleation mechanism and dimension of growth. Usually, the n value increases, between the fast and slow CR, since fat crystal nucleation events tend to be more sporadic and growth takes place in more directions [17]. This relation was not verified by our data due to non isothermal establishment of SFC, which makes comparison between

Table 2 Apparent crystallisation parameters and SFC for lipid materials crystallisation under variable CR

	Fast CR	Intermediate CR	Slow CR
AMP			
Avrami constant (k, min^{-n})	0.242	0.001	(–)
Avrami exponent (n)	1.599	1.820	(–)
Induction time (min)	0.6	0.9	(–)
SFC_{∞}	88.4 ± 0.1*	84.3 ± 0.6	83.6 ± 0.5
W/A 1			
Avrami constant (k, min^{-n})	0.190	0.004	0.001
Avrami exponent (n)	2.260	1.735	1.600
Induction time (min)	0.4	4.7	47.3
SFC_{∞}	88.8 ± 0.0	88.5 ± 0.1	88.5 ± 0.1
W/A 2			
Avrami constant (k, min^{-n})	0.190	0.010	0.000
Avrami exponent (n)	1.880	1.620	1.850
Induction time (min)	0.4	1.4	41.3
SFC_{∞}	87.3 ± 0.1	87.4 ± 0.1	87.4 ± 0.1
White beeswax			
Avrami constant (k, min^{-n})	0.586	0.160	0.190
Avrami exponent (n)	1.771	1.172	0.870
Induction time (min)	0.5	0.5	0.3
SFC_{∞}	91.6 ± 0.1	90.9 ± 0.3	91.0 ± 0.2
P/S acids			
Avrami constant (k, min^{-n})	0.473	0.002	0.038
Avrami exponent (n)	1.505	2.471	1.828
Induction time (min)	0.3	1.5	1.1
SFC_{∞}	100	100	100

* ± value stands for the confidence interval at $p < 0.05$

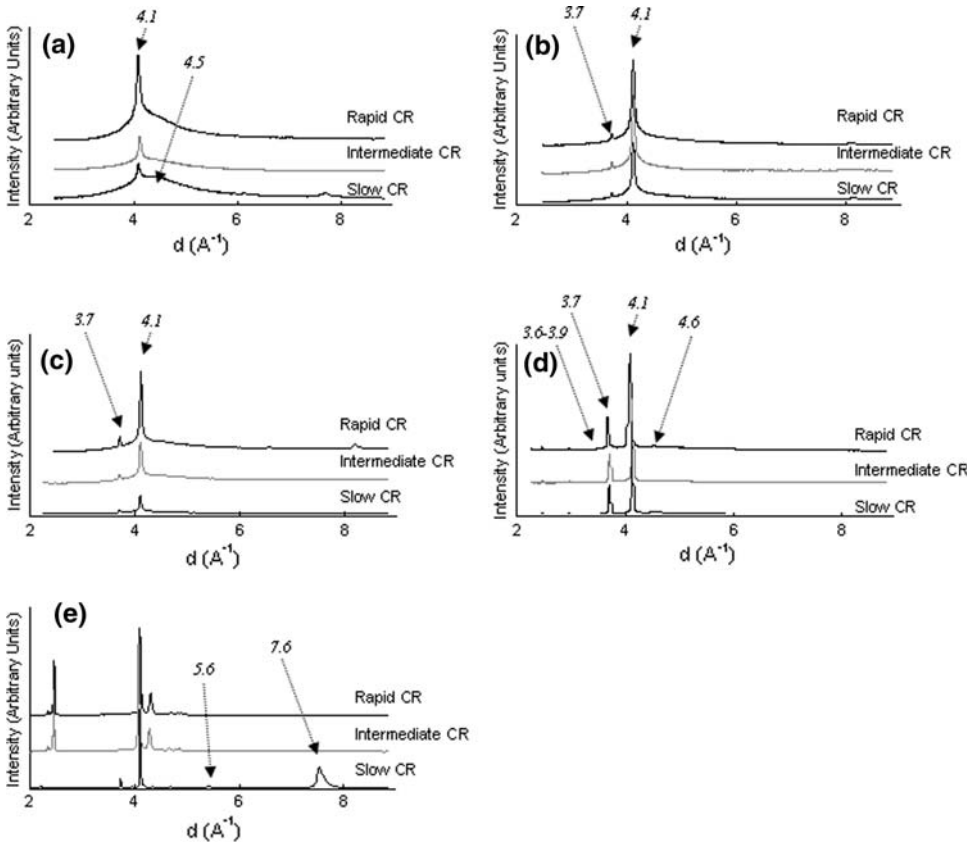

Fig. 2 Comparisons of X-ray diffraction patterns from **a** AMP film, **b** W/A 1 film, **c** W/A 2 film, **d** White beeswax, **e** P/S acids blend crystallised at either the rapid, intermediate or slow CR measured at ambient temperature

apparent kinetic parameters of crystallisation delicate. Induction times of crystallisation generally increased with the slow CR for most of the materials in our study.

These kinetic effects of CR did not have a strong impact on the final SFC_{∞}. Significant differences were noted only between the two extreme CRs, for three lipid materials out of the five studied: higher SFC_{∞} values are reached for AMP, W/A 1 and White beeswax crystallised under the rapid CR than under the slow CR. The effect on SFC_{∞} values of the different CRs varied to a large extent from more than 3% in the low MP fat to less than 0.5% in the two other fats. Similar influences of the high CR and degrees of undercooling resulting in higher SFC, with variations ranging from 0 to 10% SFC had been reported on milk fat, lard or blends of fats [16, 17]. Possible explanation for such a phenomenon reported in the literature [17] consists of a higher adsorption of liquid fat to the more numerous fat crystals induced by the rapid CR and presenting a larger specific surface. This higher adsorption would lead to a decrease in the amount of liquid fat present in the continuous phase.

Effect of CR on Lipid Crystal Habit

The XRD patterns of the five fat materials crystallised at variable CRs are presented in Fig. 2 and the corresponding polymorphs are summarised in Table 3. The polymorphic forms present in the triglyceride derivatives and beeswax were not modified by the CR. This lack of effect is confirmed by fixed melting peaks determined by DSC on the materials (Table 3). For all CRs, the AMP XRD pattern displayed: (1) a strong sharp peak centered at $d = 4.1$ Å characteristic of the α-polymorph. This polymorphic form is extremely frequent and stable for acetylated materials; (2) a strong broad peak centered at about $d = 4.5$ Å, which arises due to the scattering from the liquid phase of the sample (oil). This broad peak is the most important for the slow CR conditions for which two other small peaks at higher interplanar spacings could be observed ($d = 6.2$ and 7.7 Å). The XRD pattern of W/A 1, W/A 2 and beeswax materials present the sharp peaks ($d \sim 4.1$ Å, $d \sim 3.7$ Å) characteristic of the β' orthorhombic subcell organisation. In addition, the fraction of crystals presenting hexagonal subcell organisation in these materials can lead to an enlarged 4.1 Å peak and a decrease in the Relative Intensity (RI) ratio between the 3.7 and 4.1 Å peaks as reported by Donhowe and Fennema [11] in natural waxes presenting mixed polymorph systems. The differences in Relative Intensity ratio, presented in Table 3, inform us of the respective amount of each polymorphic form: Fast CRs induce a decrease in RI ratio for W/A 1 and W/A 2 but has no effect on the RI values reported for the White beeswax.

Table 3 Summary of water related characteristics (WVP) and physical characteristics. (Peak temperature, Tp^b determined by DSC, Polymorphic form and Relative Intensity ratio for peak intensity −3.7 Å/4.1 Å-determined by X-Ray diffraction)

Sample	$WVP^a_{0-100\%}$ (10^{-12} mol/(m s Pa))/(thickness, μm)	Tp^b (°C)	Polymorphic form	RI[c]
Fast CR				
AMP	4.91 ± 0.56[e]/(355)	30.4 ± 0.8[d]	α	0
W/A 1	2.38 ± 0.45[f]/(302)	37.5 ± 0.7[h,i]	$\beta' + \alpha$	0.15
		54.9 ± 0.3[j]		
W/A 2	0.60 ± 0.07[h]/(269)	35.4 ± 0.0[f]	$\beta' + \alpha$	0.24
		57.0 ± 0.0[l]		
White Beeswax	0.20 ± 0.10[i]/(257)	64.9 ± 0.0[o]	$\alpha + \beta' + \beta$	0.36
P/S acids	24.27 ± 7.47[d]/(341)	59.1 ± 0.2[n]	C	(–)
Intermediate CR				
AMP	3.27 ± 1.47[e,f]/(409)	30.8 ± 0.2[d]	α	0
W/A 1	1.63 ± 0.16[g]/(320)	36.6 ± 0.1[g]	$\beta' + \alpha$	0.18
		57.1 ± 3.1[j,k,l,m,n]		
W/A 2	0.57 ± 0.14[h]/(265)	35.5 ± 0.1[f]	$\beta' + \alpha$	0.26
		56.9 ± 0.2[l]		
White Beeswax	0.30 ± 0.07[i]/(290)	64.8 ± 0.1[o]	$\alpha + \beta' + \beta$	0.36
P/S acids	20.22 ± 4.64[d]/(263)	59.9 ± 1.1[n]	C	(–)
Slow CR				
AMP	6.01 ± 2.01[e]/(561)	31.4 ± 0.2[e]	α	0
W/A 1	0.61 ± 0.15[h]/(311)	38.1 ± 0.6[i]	$\beta' + \alpha$	0.20
		55.6 ± 0.2[k]		
W/A 2	0.39 ± 0.18[h,i]/(301)	36.5 ± 0.5[g,h]	$\beta' + \alpha$	0.30
		57.9 ± 0.1[m]		
White Beeswax	0.30 ± 0.04[i]/(289)	65.3 ± 0.2[o]	$\alpha + \beta' + \beta$	0.33
P/S acids	15.55 ± 6.94[d]/(324)	58.6 ± 0.2[n]	B	(–)

± Values stand for standard deviations

[a] Experimental Water Vapour Permeability determined for a 0–100% RH on self-supported structures

[b] Tp^b peak temperature determined using a DSC (2920, TA Instruments)

[c] *RI* relative intensity ratio between the intensity (counts) of the 3.7 Å and the intensity of the 4.1 Å peaks determined by powder X-Ray diffraction

[d–o] Values in columns with the same superscript letter are not significantly different ($p < 0.05$)

This value is similar to the one reported on the same material and on microcrystalline wax (formed by casting with a rapid CR 100 °C-ambient temperature). Comparatively, the lower RI ratios obtained at all CRs for W/A 1 and 2 can be related to a more important fraction of hexagonal subcell organisation in these acetylated compounds compared to the White beeswax.

In addition to the α and β' crystal fractions, the beeswax X-ray patterns for all CRs displayed a small peak at ~4.6 Å characteristic, along with other lines around 3.6–3.9 Å, of a small fraction of a β triclinic denser form of polymorph organisation. β and β' crystals are stabilised by Van Der Waals-London forces occurring between the aliphatic chains, which leads to a dense network. These forces do not exist in α form where C atoms can rotate. Thus waxes that crystallise in the orthorhombic system are much harder and less deformable than those that crystallise in the hexagonal system. This difference in molecular configuration and mechanical properties could affect the mass transfer phenomena through the barrier.

Concerning, the P/S acids blend, their polymorphic behavior follows the saturated fatty acid nomenclature and depends on the fatty acid chain length. These acids are solidified according to three main crystalline varieties: A, B and C. The associated crystalline subcells of these varieties are triclinic for the A variety, orthorhombic for the B and C forms. Conversely to the other fat materials, the XRD pattern of P/S acids blend is significantly affected by the CR: the P/S acids blend crystallised under the slow CR present a broad peak centered at $d = 7.6$ Å characterising the B orthorhombic form of the long chain fatty acids, with other peaks at $d = 5.6$ Å and $d = 49.4$ Å. For the two other CRs, this peak is not present and the fat is likely to be in the C polymorph another orthorhombic form favoured by rapid crystallisation [18].

Effect of Cooling Rate on Microstructure and Mass–Volume Related Properties

The different microstructures obtained upon slow and rapid crystallisation of W/A 1, W/A 2, AMP, White beeswax and P/S acids blend observed by polarised light microscopy are presented in Fig. 3. For all the barrier materials but the P/S acids blend, a majority of needle-like crystals presenting an anisotropic orientation can be seen. Additional platelets crystals are present in the samples containing beeswax. The P/S acids blend microstructure shows large flat crystals, more characteristic of an orthorhombic organisation.

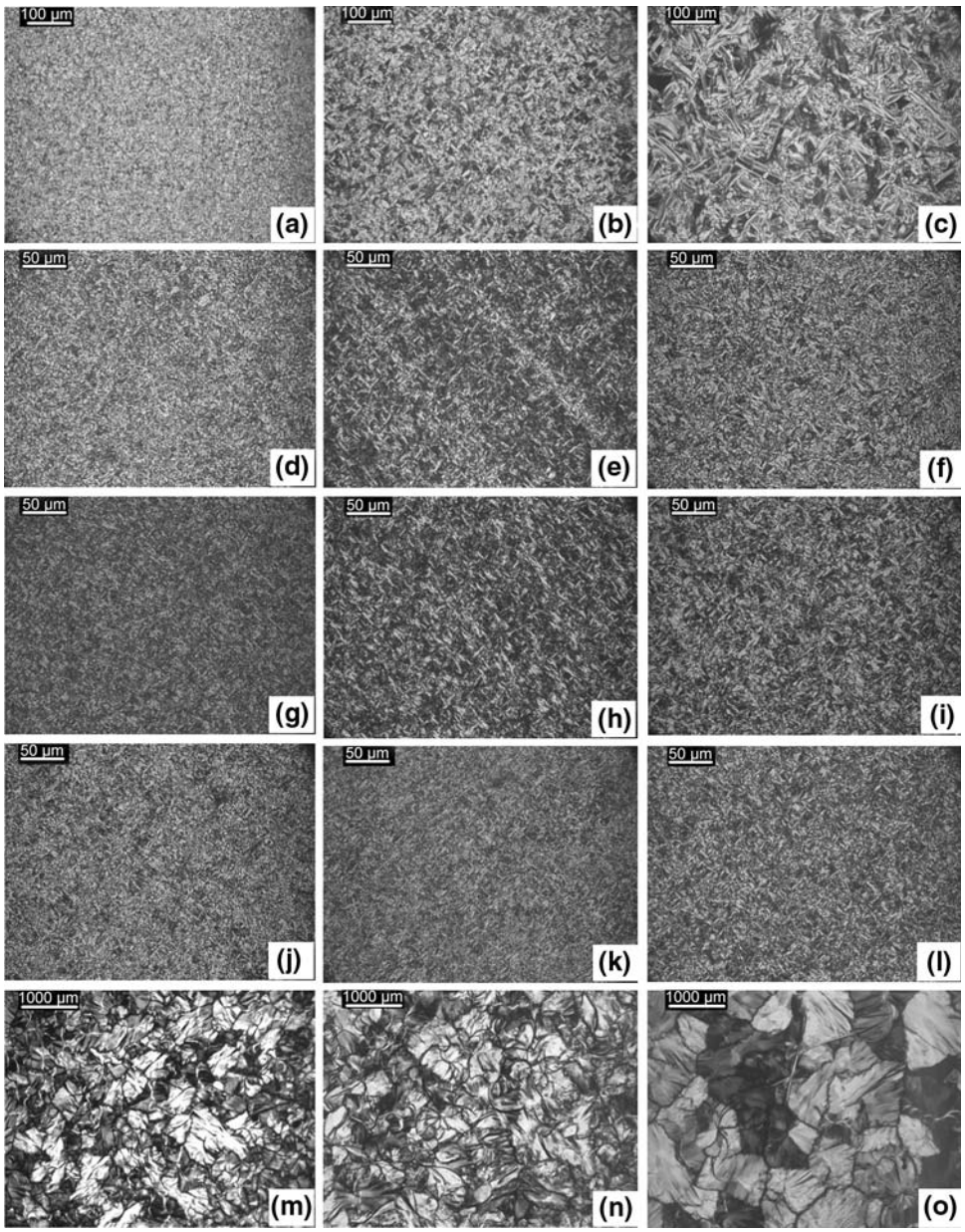

Fig. 3 Polarised light micrographs of lipid materials crystallised under different CRs: **a–c** AMP film (×200), **d–f** W/A 1 film (×400), **g–i** W/A 2 film (×400); **j–l**) White beeswax film (×400), **m–o** P/S acids blend films (×25); crystallised respectively at either the fast, intermediate or slow CR

For all the barriers obtained using the rapid CR, the microstructure of materials crystallised at an intermediate or a rapid CR showed smaller and more numerous crystals compared to barrier crystallised at a slow CR. This effect is more important on the low melting point fat (AMP) and more easily visualised on P/S acids macroscopic crystals. Dense and granular crystals morphology arose from growth processes characterised by high crystallisation and nucleation rates. The crystallisation takes place over a short period of time with instantaneous formation of a large number of nuclei. This fast crystallisation triggers a rapid increase in viscosity, thus limiting molecular diffusion and crystal growth [17]. Conversely, for a slow CR, bigger crystals and aggregates are observed. Similar results were reported on various fat materials.

On the mesoscopic scale, contact angle measurements with water were conducted to determine the surface hydrophobicity of the barrier. This surface characteristic may affect the first stage of permeation process which is generally described as a three stages mechanism: adsorption of the penetrant on the high concentration side of the film, diffusion of the penetrant through the barrier film under concentration gradient, and desorption of the penetrant on the low concentration side [4]. It is important to note that an increase in surface area by increasing surface roughness also influences the contact angle value

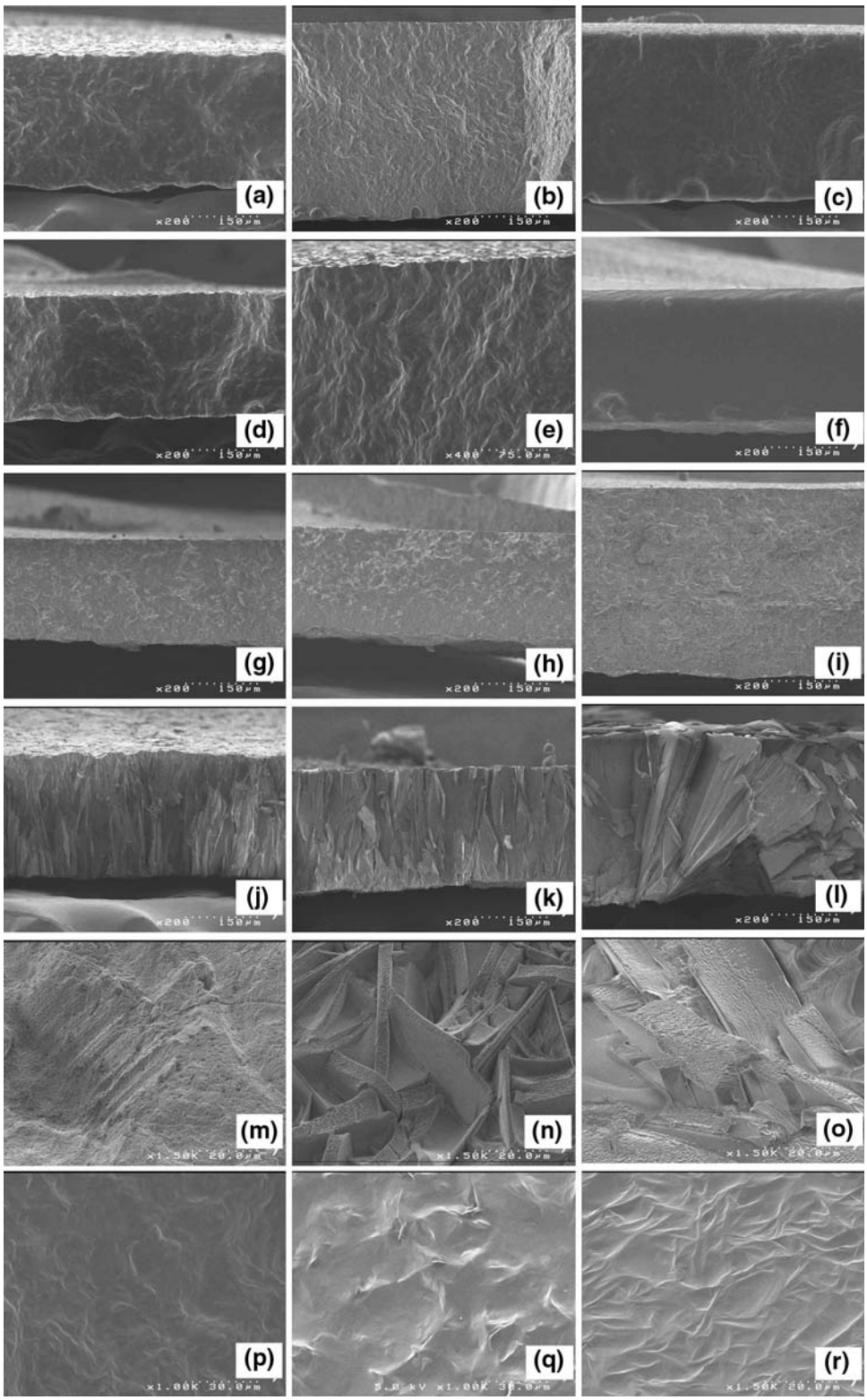

Fig. 4 SEM observations. Cryofracture cross-sections (×200): **a–c** W/A 1, **d–f** W/A 2, **g–i** White beeswax, **j–l** P/S acids films crystallised under fast, intermediate or slow CR; Surface observations (×1,500): **m–o** P/S acids films and **p–r** White beeswax crystallised under fast, intermediate or slow CR. Concerning the surface observations of W/A 1 and W/A 2, they were very comparable to the one observed for the White beeswax and therefore not included

determined [19]. The value determined on P/S acids which were the only films that presented qualitatively a significant roughness and variable surface roughness with CR (Fig. 4) can hardly be compared to the other values. The contact angles determined are presented on Fig. 5 and are characteristic of highly hydrophobic compounds (>90°) for all the material but AMP (<65°). The average value for a given material, whatever its CR, increases with its

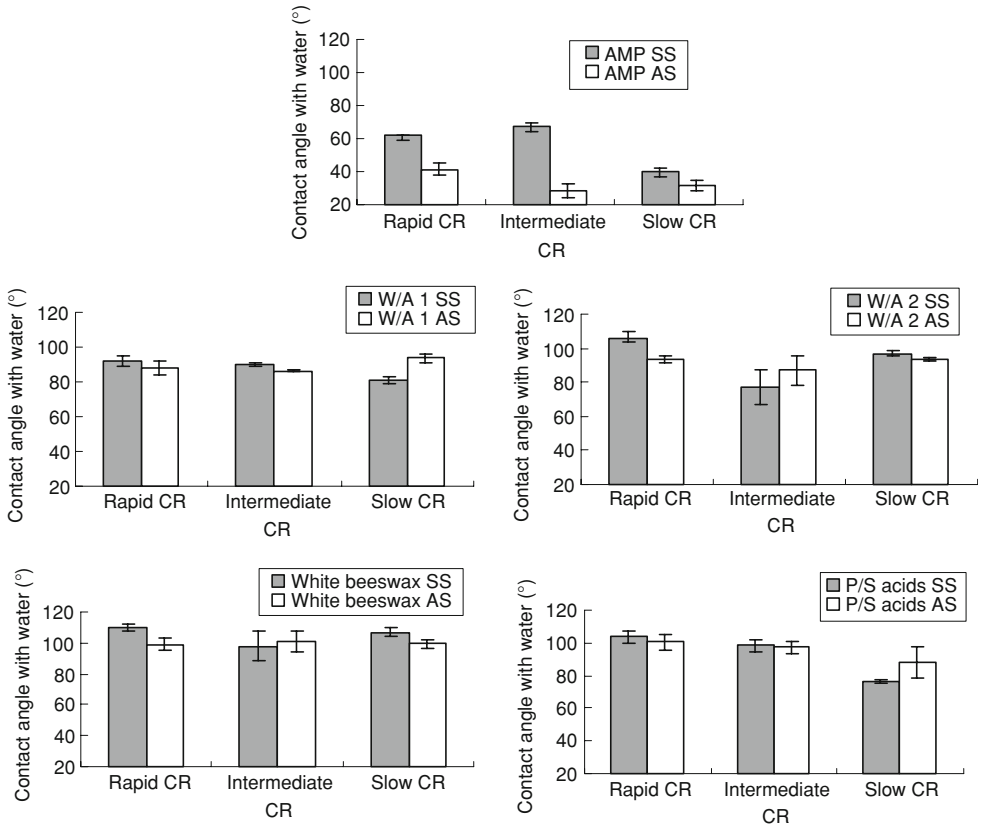

Fig. 5 Contact angle measurements with water on the five lipid-based barriers crystallised under variable CR: measurement on the two sides (*SS* support side, or *AS* air side) of the barrier (20 °C, 6 replicates)

hydrophobicity. Increasing order of hydrophobicity and increasing contact angle values coincide: AMP < W/A 1 < W/A 2 < P/S acids blend < White beeswax. CR did not seem to affect the contact angles values determined on both side of the film except for the AMP and P/S acids obtained under a slow CR. At a slow CR, these two films present lower values of contact angles. This low values can be explained (1) with regard to AMP by short chain reorganisation favoured by a slow CR, (2) with regard to P/S acids, by a decrease in surface roughness due to the formation of enlarged crystals at a slow CR (Fig. 4). In terms of polarisation (difference of contact angle value between the air side and the support side), a strong effect is noticed on AMP for the rapid and intermediate CR, and for the W/A 1 and 2 barriers respectively at slow and rapid CRs.

Mass–volume area related properties of fat materials provide information on the compactness and organisation of the fat network. However they have only been scarcely studied [18]. The effect on the film-forming technology on barrier micro-porosity was investigated measuring for each barrier its apparent density, with a classic liquid displacement pycnometric method and its true density through helium pycnometric measurements. Values for such measurements are reported on Fig. 6. No clear influence of CR on true density and apparent density values of the barrier films was determined using pycnometric methods. However, a higher variability on the measurements of films

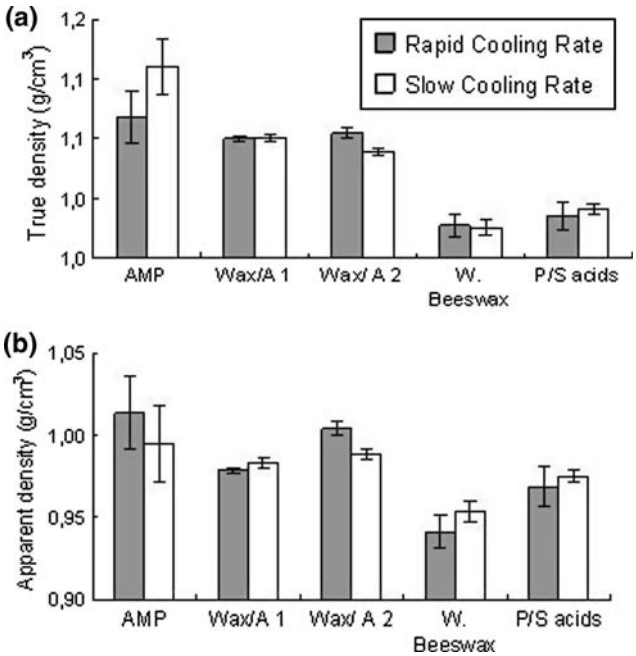

Fig. 6 Effect of CR on mass–volume related properties of the lipid films: **a** true density of the lipid films, **b** apparent density of the lipid films (20 °C, 3 replicates at least)

formed under a rapid CR was noticed. This higher variability is informative of a higher number of defects of structure in the materials obtained at such a CR. Absence

of a significant effect of the CR on the true density of the material can be linked to the lack of effect on polymorphic form present all the triglycerides studied [10]. Indeed, for triglycerides, α, β' and β polymorphs present an increasing thermodynamic stability and density: the average volume of CH_2 groups (V_{CH_2}) varies between $24.7 < V_{CH_2} < 25.7$–26 Å^3 for the α form and from 22.9 to 24.7 Å^3 for the two more compact forms. The transition between α form towards denser forms induce a decrease of V_{CH_2} of around 1–2 Å^3 due to a decrease in aliphatic chain lateral packing. This V_{CH_2} variation remains much reduced compared to a solid–liquid transition (1.5–5 Å^3). The resultant effect of polymorphic variations on the bulk density of tristearin was reported by Morillon et al. [20]: density values of 1.014, 1.017 and 1.043 g/cm^3 were observed respectively for the α, β' and β polymorphs. Very few density values of fat materials are available in the literature and, most of the time, consist of bulk density measurements. Values of 0.958–0.974 g/cm^3 (15 °C), 0.941 g/cm^3 and 1.160 g/cm^3 (20 °C) were reported respectively for White beeswax, stearic acid and glycerol triacetate [21]. A few values of self-supported cast barrier films were reported by Guillard et al. [22] using a geometric method for partially acetylated glycerides (0.890–0.908 g/cm^3, 20 °C). The range of values of apparent density in the cast self-supported films are in agreement with the previous results with average values of 0.942 and 0.957 for the White beeswax and P/S acids blend, and higher values for the barrier fat including acetyl groups (average values of 0.987–0.997 for the W/A barriers and 1.023 for AMP). Calculated porosity values (Eq. 2) are generally low for all the barriers, characteristic of dense materials, with higher values reported for AMP probably due to the presence of defects. This low porosity is confirmed by SEM cryofracture observations, which reveal a dense anisotropic structure whatever the CR for the W/A barriers and beeswax materials (Fig. 4). The roughness of the cryofracture is also indicative of the degree of crystallinity of the material. This roughness is slightly less important on the cryofracture observations of W/A barriers obtained under a slow CR than for a faster CR, confirming possible decrease in SFC. P/S acids cross-section reveals a highly crystalline barrier with isotropic organisation of platelets crystals perpendicular to the surface of the barriers and thus parallel to permeation flow.

Effect of Cooling Rate on Macroscopic Barrier Properties of the Lipid Materials

The CR did not significantly affect the WVP of the barrier films except for the W/A 1 barrier for which WVP values were negatively correlated with CRs ($r^2 > 0.99$). The slow CR induced a small but significant decrease in WVP values of W/A 1 (Table 3). Such a positive influence is difficult to correlate to the various effects of a slow CR on structural parameter of this fat material, but can be generally explained by an enhanced crystal growth, healing of film defects and polarisation of film in term of surface hydrophobicity during the slow CR. The WVP values determined on beeswax and acetylated materials are in good agreement with previous studies. For the P/S acids, which presented cracks and voids at the various CRs tested (cross-sections j, k and i on Fig. 4), moisture transfer could not be described by a permeation mechanism. The three CRs tested did not have important effect on the resulting barrier properties of the materials, though influencing its crystal size, ratio of polymorph present, SFC and the presence of defects.

Multivariable analysis of type Principal Component Analysis was conducted on the WVP data obtained at all CRs to try to determine the possible influence and

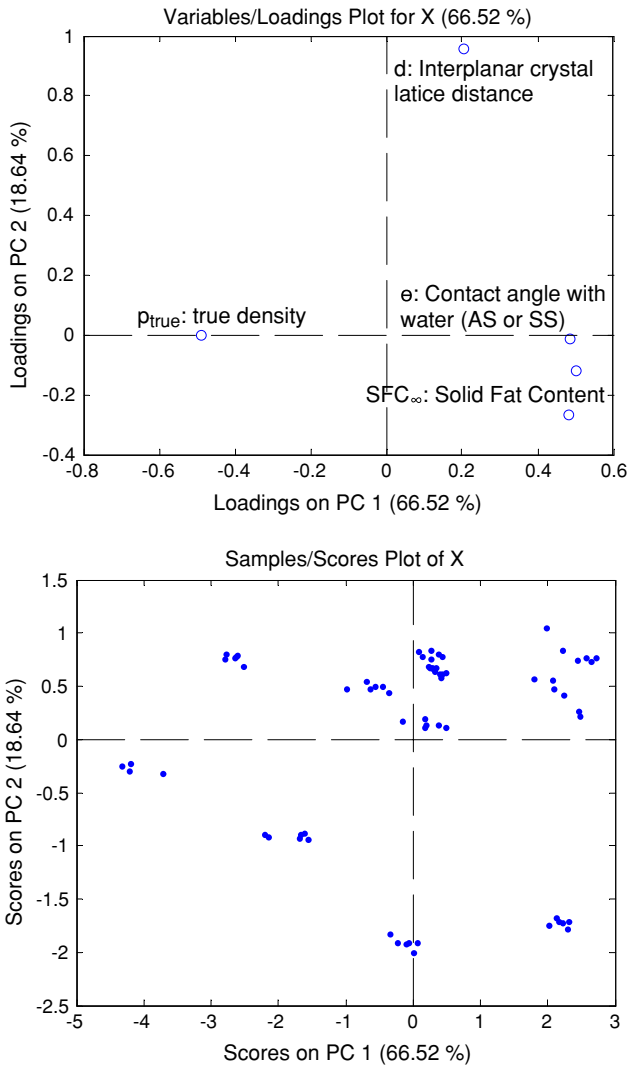

Fig. 7 Result of multivariable analysis presenting variable loadings (*above*) and samples scores (*below*) on principal component 1 and 2 determined using principal component analysis

correlations between the WVP values and the characteristics of the barrier materials determined in the present study (interplanar distance of crystals lattice, surface contact angles, true density, and SFC). The P/S acids which presented defects were excluded from the analysis. Two principal components accounted for 85% of the variance observed on data and the first component accounting for 67% of the variance on the data corresponded to the variables density and the anti-correlated variables surface contact angles and solid fat content, it can thus be considered as mainly indicative on the polarity of the material (Fig. 7). Interplanar crystal lattice distance indicative of fat polymorphism is not correlated with any of the three other variables and has less influence on WVP ($\sim$19% variance only).

Conclusion

In conclusion, the three investigated CRs triggered variable degree of undercooling in the set of fat materials, affected the size of fat crystals but had no effect on the nature of the polymorphs present except for the P/S acid blend. In W/A barriers, presenting mixed polymorph systems, a slow CR induced higher ratio of β' polymorph compared to α polymorph. Variations in CR had a limited effect on the studied meso and macroscopic properties of the barriers. The differences in values of WVP between the different materials obtained using variable CRs were mainly correlated to differences in material polarity using principal component analysis. For one barrier however (W/A 1), a slower CR favoured healing of imperfections and induced significant decrease in WVP compared to intermediate and fast CRs.

Acknowledgments We gratefully acknowledge: Nestlé Research Centre and the Product Technology Centre of York for giving financial and scientific support to this work, the Lipids Technology Unit (CIRAD) of UMR IATE for its help concerning the SFC measurements, the 'Service Commun Réseau de Rayons X et γ' (University Montpellier II) where X-Ray diffraction measurements were performed, D. Cot of the 'Institut Européen des Membranes' for SEM observations, the 'Techtonophysique Laboratoire' (University Montpellier II) for authorised use of the polarised light microscope.

References

1. McHugh TH, Krochta JM (1994) Permeability properties of edible films. In: Krochta JM, Baldwin EA, Nisperos-Carriedo MO (eds) Edible films and coatings to improve food quality. Technomic Publishing Company, Lancaster, pp 139–187
2. Shellhammer TH, Rumsey TR, Krochta JM (1997) Viscoelastic properties of edible lipids. J Food Eng 33:305–320
3. Morillon V, Debeaufort F, Blond G, Capelle M, Voilley A (2002) Factors affecting the moisture permeability of lipid-based edible films: a review. Crit Rev Food Sci Nutr 42:67–89
4. Bourlieu C, Guillard V, Powell H, Vallès-Pàmies B, Guilbert S, Gontard N (2009) Edible moisture barriers: how to assess of their potentials and limits in food products shelf-life extension? Crit Rev Food Sci Nutr 49:474–499
5. Guillard V, Guillbert S, Bonazzi C, Gontard N (2004) Edible acetylated monoglyceride films: effect of film-forming technique on moisture barrier properties. J Am Oil Chem Soc 81:1053–1058
6. Bourlieu C, Ferreira M, Barea B, Guillard V, Villeneuve P, Guilbert S, Gontard N (2009) Moisture barrier and physical properties of acetylated derivatives with increasing acetylation degree. Eur J lipid Sci Techn 111(5):489–498
7. Martin-Polo M, Mauguin C, Voilley A (1992) Hydrophobic films and their efficiency against moisture transfer. 1. Influence of the film preparation technique. J Agric Food Chem 40:407–412
8. Lovegren NV, Feuge RO (1954) Permeability of acetostearin products to water vapor. J Agric Food Chem 2:558–563
9. Landmann W, Lovegren NV, Feuge RO (1960) Permeability of some fat products to moisture. J Am Oil Chem Soc 37(1):1–4
10. Kester JJ, Fennema O (1989) The influence of polymorphic form on oxygen and water-vapor transmission through lipid films. J Am Oil Chem Soc 66:1147–1153
11. Donhowe IG, Fennema O (1993) Water-vapor and oxygen permeability of wax films. J Am Oil Chem Soc 70:867–873
12. Sato K (2001) Crystallization behaviour of fats and lipids—a review. Chem Eng Sci 56:2255–2265
13. Fox RC (1958) The relationship of wax crystal structure to the water vapor transmission rate of wax films. TAPPI 41:283–289
14. Kester JJ, Fennema O (1989) Tempering influence on oxygen and water vapor transmission through a stearyl alcohol film. J Am Oil Chem Soc 66:1154–1157
15. Martini S, Kim DA, Ollivon M, Marangoni AG (2006) Structural factors responsible for the permeability of water vapor through fat barrier films. Food Res Int 39:550–558
16. Martini S, Kim DA, Ollivon M, Marangoni AG (2006) The water vapor permeability of polycrystalline fat barrier films. J Agric Food Chem 54:1880–1886
17. Campos R, Narine SS, Marangoni AG (2002) Effect of cooling rate on the structure and mechanical properties of milk fat and lard. Food Res Int 35:971–981
18. Ollivon M, Perron R (1992) Chapitre IV. Propriétés chimiques des corps gras. In: Karleskind A (ed) Manuel des corps gras. Tec & Doc, Lavoisier, Paris, pp 433–529
19. Burton Z, Bhushan B (2006) Surface characterization and adhesion and friction properties of hydrophobic leaf surfaces. Ultramicroscopy 106:709–719
20. Morillon V, Debeaufort F, Capelle M, Blond G, Voilley A (2000) Influence of the physical state of water on the barrier properties of hydrophilic and hydrophobic films. J Agric Food Chem 48:11–16
21. Lide DR (1972) Handbook of chemistry and physics. 53rd edn. CRC (Chemical Rubber Company) Press, Cleveland
22. Guillard V, Broyart B, Bonazzi C, Guilbert S, Gontard N (2003) Preventing moisture transfer in a composite food using edible films: Experimental and mathematical study. J Food Sci 68:2267–2277